

Interlayer Interactions in $M(\text{OH})_2$: A Neutron Diffraction Study of $\text{Mg}(\text{OH})_2$ L. DESGRANGES,^a G. CALVARIN^a AND G. CHEVRIER^b^aLaboratoire de Chimie-Physique du Solide, URA CNRS 453, Ecole Centrale de Paris, 92295 Châtenay-Malabry CEDEX, France, and ^bLaboratoire Léon Brillouin, CEA-CNRS, CEN Saclay, 91191 Gif-sur-Yvette CEDEX, France

(Received 15 April 1995; accepted 21 June 1995)

Abstract

Magnesium hydroxide, $\text{Mg}(\text{OH})_2$: $M_r = 58.3$, trigonal, $P3m1$, $a = 3.148$ (1), $c = 4.779$ (2) Å, $V = 41.015$ Å³, $D_x = 2.36$ g cm⁻³ at room temperature; $a = 3.145$ (1), $c = 4.740$ (2) Å, $V = 40.602$ Å³, $D_x = 2.39$ g cm⁻³ at 70 K; $Z = 1$, $\lambda = 0.8330$ (5) Å, $\mu = 1.78$ cm⁻¹, $F(000) = 9.503$ fm; final $R = 2.42$, $wR = 2.40$, $S = 3.22$ for 82 unique reflections at room temperature; $R = 1.84$, $wR = 1.82$, $S = 2.54$ for 81 unique reflections at 70 K. Refinements have been carried out using anisotropic thermal coefficients for all atoms. To interpret the very large thermal motion of the H atom, subsequent refinements have been carried out with an anharmonic model and with a three-site split-atom model, and results are compared with those previously reported for $\text{Ca}(\text{OH})_2$. By comparing the interatomic distances O...O, H...H and H...O in the interlayer spacing of $\text{Mg}(\text{OH})_2$ and $\text{Ca}(\text{OH})_2$, as well as their temperature dependence, the nature and the strength of interlayer interactions in both compounds are discussed.

1. Introduction

Brucite $\text{Mg}(\text{OH})_2$ belongs to the family of divalent metal hydroxides $M(\text{OH})_2$, with $M = \text{Mg}, \text{Ca}, \text{Ni}, \text{Co}, \text{Fe}, \text{Mn}$ or Cd , which are isostructural with the layered compound CdI_2 (space group $P3m1$). In $M(\text{OH})_2$ compounds the layers are built with distorted edge-sharing MO_6 octahedra, the M cation planes being situated between alternate pairs of O planes which form an almost hexagonal close-packed array. The hydroxyl groups (OH), which are directed along the threefold axes, are bonded to three M cations and in interlayer spacings they are surrounded by three other (OH) groups belonging to the adjacent layer (Fig. 1).

Hydroxides $M(\text{OH})_2$ are of special interest for studying the influence of the cation M (nature, ionic radius) on structural packing and IR (OH) stretching frequencies in solids, owing to their crystalline structure which is comparatively simple (Brindley & Kao, 1984). On the other hand, the nature of the interactions between adjacent layers has been the subject of controversy in the literature; recently, Krüger, Williams & Jeanioz (1989) reported the presence of hydrogen bonding in

$\text{Mg}(\text{OH})_2$ and $\text{Ca}(\text{OH})_2$ from IR spectroscopy experiments under pressure.

An early structural study of an hydroxide $M(\text{OH})_2$, by single-crystal neutron diffraction, was carried out by Busing & Levy (1957) on $\text{Ca}(\text{OH})_2$. They reported an unusual thermal motion for the H atom; it is very large and anisotropic at room temperature as well as low temperature (130 K). The authors suggested that the H atom undergoes a 'riding' motion and proposed a mathematical expression, based on an umbrella-shaped distribution for the H atom, to calculate the actual O—H bond length. This unusual thermal behavior has since been revealed in other hydroxides: $\text{Mg}(\text{OH})_2$ (Zigan & Rothbauer, 1967) and $\text{Ni}(\text{OH})_2$ (Greaves & Thomas, 1986). In a recent study (Desgranges *et al.*, 1993), we analyzed more precisely the thermal motion of the H atom in $\text{Ca}(\text{OH})_2$ using more accurate and more fully extended neutron data sets collected at 80 K and room temperature. Thus, for the first time, refinements with an anharmonic thermal motion model for the H atom could be performed. Comparison between 80 K and room temperature results led us to propose a three-site split-atom model for the H atom, which enables to describe more satisfactorily the H-atom thermal motion.

The crystal structure of $\text{Mg}(\text{OH})_2$ was first refined by Zigan & Rothbauer (1967), but in this work the calculated value for the O—H bond length is much

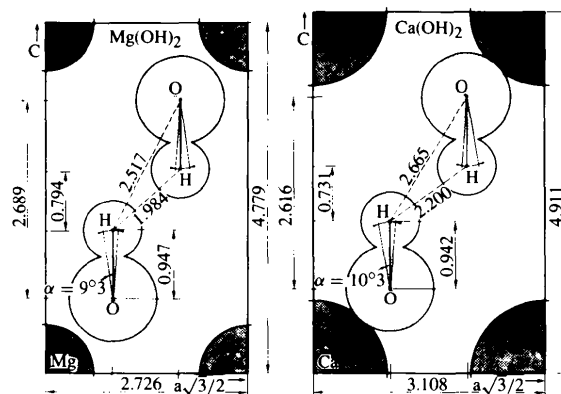


Fig. 1. Structure of $\text{Mg}(\text{OH})_2$ and $\text{Ca}(\text{OH})_2$ in projection in the plane ($a + b/2, c$). Numerical values correspond to the room temperature results.

larger than in $\text{Ca}(\text{OH})_2$ and $\text{Ni}(\text{OH})_2$. Recently, the crystal structure of deuterated brucite $\text{Mg}(\text{OD})_2$ has been refined at room temperature from time-of-flight powder neutron diffraction data (Partin, O'Keeffe & Von Dreele, 1994). The calculated O—D bond length, corrected for 'riding' motion (0.956 Å), agrees well with the O—H bond in $\text{Ca}(\text{OH})_2$ and $\text{Ni}(\text{OH})_2$.

The aim of this study is to improve the description of H-atom thermal motion in $\text{Mg}(\text{OH})_2$ from single-crystal neutron diffraction data collected at room temperature and 70 K. Structural refinements were carried out, using the same thermal motion models as for $\text{Ca}(\text{OH})_2$, and the results are discussed and compared.*

2. Experimental

An untwinned part was cut from a natural crystal of $\text{Mg}(\text{OH})_2$. The unit-cell parameters and the orientation matrix were refined using 20 centered reflections. Bragg intensities were measured normally for three symmetry-equivalent reflections, with $\lambda = 0.8330$ (5) Å, on a neutron four-circle P110 diffractometer at the Orphee Reactor (CEN-Saclay). For the data collections, ω scans ($3 \leq 2\theta \leq 75^\circ$) and $\omega-2\theta$ scans ($75 \leq 2\theta \leq 77.6^\circ$) were used; 41 steps, 2.5–5 s per step as a function of $I/\sigma(I)$ of scan widths according to the instrumental resolution ($195-658 \text{ tg}\theta + 1072 \text{ tg}^2\theta$)°.

The sample was mounted in a He cryostat and two data sets were collected at room temperature (324 reflections measured, $\sin \theta/\lambda \leq 0.763$, good stability of the standard reflections 004 and $\bar{2}1\bar{2}$) and 70 K (202 reflections measured, $\sin \theta/\lambda \leq 0.716$).

The integrated intensities were determined from resolution-adapted profile measurement of the peaks. The background was calculated from an average of the first and last steps of each side of the reflections: Lorentz-polarization and absorption corrections were performed; no extinction correction was applied because of the large mosaic spread of the used crystal.

Refinements were performed on a SUN 4-370 computer, using the full-matrix least-squares method based on F , with the program *PROMETHEUS* (Zucker, Perenthaler, Kuhs, Backmann & Schulz, 1983). The neutron scattering lengths for Mg, O and H were taken as $b_{\text{Mg}} = 5.375$, $b_{\text{O}} = 5.805$ and $b_{\text{H}} = -3.741$ fm (Delapalme, 1985). Table 1 provides full experimental details.

3. Refinements

The atomic positions of Mg, O and H in the space group $P\bar{3}m1$ are, respectively, $1(a)$ (0, 0, 0), $2(d)$ ($\frac{1}{3}, \frac{2}{3}, z$) and

$2(d)$ ($\frac{1}{3}, \frac{2}{3}, z$). There are two independent anisotropic thermal coefficients, u_{11} and u_{33} , for all the atoms in an harmonic model of thermal motion. As for $\text{Ca}(\text{OH})_2$, refinements have also been carried out with an anharmonic model and with a three-site split-atom model for the H atom.

Results of refinements with a harmonic thermal motion model (nine parameters refined) are given in Table 2 and compared with those of $\text{Ca}(\text{OH})_2$. The values of u_{ij} coefficients are very close for both compounds; however, for $\text{Mg}(\text{OH})_2$ thermal motion is slightly less anisotropic for Mg and H, but is more anisotropic for O.

In the anharmonic thermal motion model, the coefficients were developed in a Gram-Charlier expansion up to fourth order. Since the site symmetry of the H atom is $3m$, there are three third-order and four fourth-order independent anharmonic coefficients. The total number of refined parameters is 16. Results are given in Table 3. Unlike $\text{Ca}(\text{OH})_2$, all the anharmonic coefficients are below 3σ and consequently their values are not statistically meaningful. This result could be due to data sets which are less $\sin \theta/\lambda$ extended for $\text{Mg}(\text{OH})_2$: 72 and 57 reflections, with $F^2 > 2.5\sigma(F^2)$, at room temperature and 70 K, respectively, against 188 and 88, with $F^2 > 3\sigma(F^2)$, for $\text{Ca}(\text{OH})_2$.

In the three-site split-atom model, each H atom ($\frac{1}{3}, \frac{2}{3}, z$) is split into three positions $6(i)$ (x, \bar{x}, z) with an equal occupation rate. The number of refined parameters is 12, of which four are anisotropic thermal coefficients for the H atom in a harmonic model. Results are given in Table 4. In this model the O—H direction makes an angle α with the threefold c axis (Fig. 1). The calculated values are $7.8(2)$ and $9.3(2)^\circ$ at 70 K and room temperature, respectively, and are very close to those of $\text{Ca}(\text{OH})_2$, 9.9 and 10.3° at 80 K and room temperature, respectively.

4. Discussion

The bond lengths Mg—O and O—H, interatomic distances $\text{O} \cdots \text{O}$, $\text{H} \cdots \text{H}$ and $\text{H} \cdots \text{O}$, bond angle $\beta = \text{O}—\text{M}—\text{O}$ and the valence angle $\gamma = \text{O}—\text{H} \cdots \text{O}$, as well as the a and c unit-cell parameters of $\text{Mg}(\text{OH})_2$ are given in Table 5 with the corresponding values for $\text{Ca}(\text{OH})_2$. The values of the distances O—H, $\text{H} \cdots \text{H}$ and $\text{H} \cdots \text{O}$ and of the angle γ are given both for the harmonic one-site model (1) and the three-site model (3).

For both compounds the cation-oxygen distance ($M—O$) is exactly equal to the sum of the effective ionic radii for cations M^{VI} in sixfold coordination and oxygen ions O^{IV} in fourfold coordination [2.10 Å for Mg—O and 2.38 Å for Ca—O, from Shannon (1974)]. The bond angle $\beta = \text{O}—\text{M}—\text{O}$ in the octahedral sheets, where the O ions are in the same plane, is almost constant for all the $M(\text{OH})_2$ structures with an average value $\beta = 97.4(4)^\circ$; it results that the a unit-cell

* The numbered intensity of each measured point on the profile has been deposited with the IUCr (Reference: DU0401). Copies may be obtained through The Managing Editor, International Union of Crystallography, 5 Abbey Square, Chester CH1 2HU, England.

Table 1. *Experimental details*

	Room temperature data	Data at 70 K
Crystal data		
Chemical formula	H_2MgO_2	H_2MgO_2
Chemical formula weight	58.3	58.3
Cell setting	Trigonal	Trigonal
Space group	$P\bar{3}m1$	$P\bar{3}m1$
a (Å)	3.148 (1)	3.145 (1)
c (Å)	4.779 (2)	4.740 (2)
V (Å ³)	41.015	40.602
Z	1	1
D_x (Mg m^{-3})	2.36	2.39
Radiation type	Neutron	Neutron
Wavelength (Å)	0.8330 (5)	0.8330 (5)
No. of reflections for cell parameters	20	20
θ range (°)	12–30	12–30
μ (mm^{-1})	0.178	0.178
Temperature (K)	298	70
Crystal form	Platelet	Platelet
Crystal size (mm)	$5.6 \times 5.4 \times 0.6$	$5.6 \times 5.4 \times 0.6$
Crystal color	Colorless	Colorless
Data Collection		
Diffractionmeter	P110 Canal 5C2	P110 Canal 5C2
Data collection method	ω - 2θ	ω - 2θ
Absorption correction	Empirical	Empirical
T_{min}	0.5401	0.5414
T_{max}	0.8979	0.8979
No. of measured reflections	324	202
No. of independent reflections	82	81
No. of observed reflections	72	57
Criterion for observed reflections	$F^2 > 2.5\sigma(F^2)$	$F^2 > 2.5\sigma(F^2)$
R_{int}	0.044	0.046
θ_{max} (°)	33.46	36.61
Range of h, k, l	$0 \rightarrow h \rightarrow 4$ $0 \rightarrow k \rightarrow 4$ $0 \rightarrow l \rightarrow 7$	$0 \rightarrow h \rightarrow 4$ $0 \rightarrow k \rightarrow 4$ $0 \rightarrow l \rightarrow 7$
No. of standard reflections	2	2
Frequency of standard reflections	Every 2 h	Every 2 h
Intensity decay (%)	1	1
Refinement		
Refinement on	F	F
R	2.42	1.84
wR	2.40	1.82
S	3.22	2.54
No. of reflections used in refinement	82	81
No. of parameters used	12	12
H-atom treatment	See text	See text
Weighting scheme	$w = 1/\sigma^2$	$w = 1/\sigma^2$
$(\Delta/\sigma)_{\text{max}}$	0.0	0.0
$\Delta\rho_{\text{max}}$ (e Å^{-3})	0.612	0.447
$\Delta\rho_{\text{min}}$ (e Å^{-3})	-0.334	-0.423
Extinction method	None	None
Source of atomic scattering factors	Delapalme (1985)	Delapalme (1985)

parameter of these compounds is linearly related to the (M —O) bond length (Brindley & Kao, 1984). Likewise, the thickness of the octahedral sheets c_o (distance between the oxygen planes, Table 5 and Fig. 1) is fully determined by the (M —O) bond length and the angle β (Brindley & Kao, 1984). On the other hand, the plot of the interlayer distance c_i ($c = c_o + c_i$, Fig. 1) versus M —O provides evidence for two distinct groups for the $M(\text{OH})_2$ compounds: one for the rare gas-type cation Mg^{2+} and Ca^{2+} and the other for the transition metal cations (Brindley & Kao, 1984). Using an O—H distance of 0.995 Å in $\text{Mg}(\text{OH})_2$ and of 0.936 Å in $\text{Ca}(\text{OH})_2$, the authors interpreted the decrease in c_i from $\text{Mg}(\text{OH})_2$ to $\text{Ca}(\text{OH})_2$ ($\Delta c_i = 0.073$ Å at room tempera-

ture) by the O—H bond length. Our results disagree with this interpretation because these bond lengths are equal, taking into account the standard deviation, for $\text{Mg}(\text{OH})_2$ and $\text{Ca}(\text{OH})_2$, both for the one-site (1) and the three-site (3) models (Table 5).

Although the distance c_i and, consequently, the distance between H planes, are slightly longer for $\text{Mg}(\text{OH})_2$, the interatomic distances $\text{H} \cdots \text{H}$ and $\text{H} \cdots \text{O}$ are much shorter (Table 5), for example, 1.984 against 2.200 Å for the $\text{H} \cdots \text{H}$ distance in the one-site model (1) at room temperature. This results from the distance between O—H groups in octahedral sheets, which is shorter in the $\text{Mg}(\text{OH})_2$ structure [3.148 against 3.589 Å for $\text{Ca}(\text{OH})_2$]. In the three-site model (3) each H atom is

Table 2. Results of the refinements with a harmonic thermal motion model and comparison with $\text{Ca}(\text{OH})_2$ (from Desgranges et al., 1993)

	70 K $\text{Mg}(\text{OH})_2$	80 K $\text{Ca}(\text{OH})_2$	Room temperature	
			$\text{Mg}(\text{OH})_2$	$\text{Ca}(\text{OH})_2$
z_{O}	-0.2195 (2)	-0.2341 (1)	-0.2187 (2)	-0.2337 (1)
z_{H}	-0.4205 (5)	-0.4285 (3)	-0.4169 (5)	-0.4256 (2)
M	u_{11}	47 (4)	16 (2)	61 (4)
	u_{33}	100 (7)	62 (4)	165 (8)
	B_{eq}	0.51	0.25	0.75
				0.60
O	u_{11}	48 (3)	32 (2)	74 (3)
	u_{33}	98 (6)	49 (3)	133 (5)
	B_{eq}	0.51	0.30	0.74
				0.71
H	u_{11}	347 (8)	346 (4)	484 (10)
	u_{33}	145 (10)	107 (5)	181 (11)
	B_{eq}	2.21	2.10	3.03
				3.10
R	0.019	0.019	0.025	0.028
wR	0.020	0.020	0.025	0.029

Thermal coefficients u_{ij} are given in $\text{\AA}^2 \times 10^4$ and equivalent isotropic parameters B_{eq} in \AA^2 .

Table 3. Results of the refinements with an anharmonic thermal motion model for the H atom

	70 K	Room temperature
z_{O}	-0.2190 (4)	-0.2189 (3)
z_{H}	-0.4222 (13)	-0.4167 (12)
Mg	u_{11}	41 (4)
	u_{33}	104 (7)
	B_{eq}	0.49
		0.75
O	u_{11}	50 (3)
	u_{33}	74 (9)
	B_{eq}	0.46
		0.73
H	u_{11}	359 (22)
	u_{33}	161 (41)
	c_{111}	-0.0012 (8)
	c_{333}	-0.0011 (5)
	c_{113}	0.0012 (4)
	d_{1111}	0.0002 (5)
	d_{3333}	0.00006 (11)
	d_{1113}	0.00010 (11)
	d_{1133}	0.00013 (7)
	B_{eq}	2.31
	R	0.017
	wR	0.016

Thermal coefficients u_{ij} are given in $\text{\AA}^2 \times 10^4$ and equivalent isotropic parameters B_{eq} in \AA^2 .

moved towards one O—H group of the adjacent layer such that there are one $\text{H} \cdots \text{H}$ distance and one $\text{H} \cdots \text{O}$ distance shorter and two distances longer (Table 5).

The single crystals of $\text{Ca}(\text{OH})_2$ can be easily cleaved, so Busing & Levy (1957) considered that the interlayer cohesion in this compound would be due to van der Waals interactions. This assumption cannot be applied to $\text{Mg}(\text{OH})_2$, because the $\text{H} \cdots \text{H}$ distance is much too short (1.984 Å at room temperature) compared with the usual value for a van der Waals bond (around 2.4 Å); moreover, the easy cleavage of $\text{Ca}(\text{OH})_2$ crystals, due to a weak resistance to shear stress, does not necessarily involve weak interlayer cohesion.

The strength of atomic interactions can be estimated from values of thermal expansion coefficients; a strong ionocovalent interaction leads to low values of thermal

Table 4. Results of the refinements with a three-site split-atom model for the H atom

	70 K	Room temperature
z_{O}	-0.2194 (2)	-0.2187 (2)
x_{H}	0.3569 (9)	0.3616 (9)
z_{H}	-0.4195 (6)	-0.4161 (7)
Mg	u_{11}	46 (4)
	u_{33}	99 (7)
	B_{eq}	0.50
O	u_{11}	50 (3)
	u_{33}	93 (6)
	B_{eq}	0.51
H	u_{11}	254 (22)
	u_{33}	149 (10)
	u_{12}	112 (39)
	u_{13}	-64 (24)
	B_{eq}	1.78
R	0.018	
wR	0.018	

Thermal coefficients u_{ij} are given in $\text{\AA}^2 \times 10^4$ and equivalent isotropic parameters B_{eq} in \AA^2 .

Table 5. Unit-cell parameters a and c , layer and interlayer thickness c_o and c_i , bond lengths $M—O$ and $O—H$, interatomic distances $O \cdots O$, $H \cdots H$ and $H \cdots O$, valence angle $\beta = O—M—O$ and angles $\alpha = (O—H, c)$ and $\gamma = (O—H \cdots O)$ for $\text{Mg}(\text{OH})_2$ and $\text{Ca}(\text{OH})_2$, calculated both with a one-site model (1) and a three-site model (3)

	$\text{Mg}(\text{OH})_2$		$\text{Ca}(\text{OH})_2$	
	70 K	Room temperature	80 K	Room temperature
a (Å)	3.145 (1)	3.148 (1)	3.583 (9)	3.589 (8)
c (Å)	4.740 (2)	4.779 (2)	4.894 (15)	4.911 (14)
c_o (Å)	2.081	2.090	2.291	2.295
c_i (Å)	2.659	2.689	2.603	2.616
$M—O(1)$	2.093 (4)	2.097 (3)	2.367 (4)	2.371 (3)
$O—H(1)$	0.953 (3)	0.947 (3)	0.950 (3)	0.942 (2)
(3)	0.957 (4)	0.956 (4)	0.959 (3)	0.949 (2)
$O \cdots O(1)$	3.220 (6)	3.245 (4)	3.323 (6)	3.338 (6)
$H \cdots H(1)$	1.966 (3)	1.984 (3)	2.187 (4)	2.200 (3)
$H \cdots O(1)$	1.914 (5)	1.921 (5)	2.117 (7)	2.131 (5)
$H \cdots H(3)$	2.088 (5)	2.128 (5)	2.347 (7)	2.366 (5)
$H \cdots H \times 2$	2.100 (5)	2.145 (5)	2.364 (7)	2.384 (5)
$H \cdots O(1)$	2.492 (5)	2.517 (4)	2.648 (5)	2.665 (3)
$H \cdots O(3)$	2.404 (5)	2.411 (4)	2.524 (5)	2.541 (4)
$H \cdots O \times 2$	2.545 (5)	2.579 (5)	2.179 (6)	2.741 (4)
β (°) (1)	97.4	97.3	98.4	98.4
α (°) (3)	7.8	9.3	9.9	10.3
γ (°) (1)	133.2	133.8	128.4	128.9
(3)	143.0	145.6	140.8	141.7
$\times 2$	127.7	127.0	121.6	121.6

expansion (typically around $10 \times 10^{-6} \text{ K}^{-1}$), while a weak van der Waals interaction leads to values typically around $100 \times 10^{-6} \text{ K}^{-1}$ (Krishnan, Srinivasan & Devanarayanan, 1979). For the $\text{Mg}(\text{OH})_2$ and $\text{Ca}(\text{OH})_2$ compounds, the thermal expansion in the layer planes is very low, 7.8 and $4.2 \times 10^{-6} \text{ K}^{-1}$, respectively, which is due to the strong ionocovalent $M—O$ bonds, of which the length decreases very little as temperature is lowered (Table 5). Along the c axis, orthogonally to the layers, the thermal expansion α_c is 36 and $16 \times 10^{-6} \text{ K}^{-1}$ for $\text{Mg}(\text{OH})_2$ and $\text{Ca}(\text{OH})_2$, respectively. In the interlayer spacing, the thermal expansion $\alpha_c = \Delta c / c_i \Delta T$ is directly correlated to the temperature dependence of the

interatomic distances $\text{H}\cdots\text{H}$ and $\text{H}\cdots\text{O}$, 50 and $23 \times 3 \cdot 10^{-6} \text{ K}^{-1}$, respectively, for $\text{Mg}(\text{OH})_2$ and $\text{Ca}(\text{OH})_2$. These values show that the interlayer cohesion cannot be considered weak, particularly for $\text{Ca}(\text{OH})_2$.

In order to interpret these relatively low values, it can be thought that the interlayer cohesion is realized by electrostatic interactions; in such a case the layer packing results from an equilibrium between the $\text{H}\cdots\text{H}$ repulsions and the $\text{H}\cdots\text{O}$ attractions. Results obtained with the three-site split-atom model are in agreement with this assumption, because one $\text{H}\cdots\text{O}$ distance is decreased [2.411 against 2.517 Å for the one-site model, for $\text{Mg}(\text{OH})_2$ at room temperature] and two distances $\text{H}\cdots\text{H}$ are increased (Table 5). Making the rough approximation that charges for O and H atoms are -2 and $+1$, respectively, the electrostatic bonding energy between layers can be calculated, considering only the $\text{H}\cdots\text{H}$ and $\text{H}\cdots\text{O}$ interactions. The calculated value is slightly lower for $\text{Ca}(\text{OH})_2$ (ca 2%), which means that the interlayer cohesion should be greater in this compound, in agreement with the experimental results concerning the thermal expansion of the interlayer spacing. However, a purely ionic interaction model must be considered with caution, because the $\text{H}\cdots\text{O}$ distances are such that a slight overlap of electronic clouds cannot be neglected, which should involve an interaction similar to weak hydrogen bonding.

Kruger, Williams & Jeanioz (1989) reported that the frequency of the IR-active (A_{2u}) mode of $\text{Mg}(\text{OH})_2$ and $\text{Ca}(\text{OH})_2$ decreases with pressure, by 0.6 and $3.5 \text{ cm}^{-1} \text{ GPa}^{-1}$, respectively. The authors explained the negative pressure dependence of this mode in terms of compression increasing the hydrogen-bond strength within the hydroxide structure; the hydrogen bonding exists even at zero pressure.

Usually the hydrogen bonding is divided into two classes according to the $\text{O}\cdots\text{O}$ distance, short (or strong) bonds, between 2.4 and 2.75 Å, which are essentially linear with $\gamma \approx 170^\circ$, and long (or weak) bonds, with a reduced value for γ . In the last case the hydrogen bonding is often bifurcated, *i.e.* the H-atom has two near O in approximately the same plane (Ceccarelli, Jeffrey & Taylor, 1981). In the $M(\text{OH})_2$ structures, each O—H group is surrounded by three other hydroxyl groups belonging to the adjacent layer; thus, the hydrogen bonding is trifurcated according to the previous terminology. In the one-site model the three distances $\text{O}\cdots\text{H}\cdots\text{O}$ and the three angles γ with the adjacent OH groups are equal; on the other hand, in the three-site model one distance is shortened and the corresponding γ angle is increased (Table 5) which strengthens one hydrogen bonding.

5. Concluding remarks

The temperature dependence of the interatomic distances in $\text{Mg}(\text{OH})_2$ and $\text{Ca}(\text{OH})_2$ indicates that the interlayer

cohesion can be explained by the existence of weak hydrogen bonding and that this bonding is slightly weaker for $\text{Ca}(\text{OH})_2$. This result is in agreement with the respective values of frequency changes as a function of pressure reported by Kruger, Williams & Jeanioz (1989) for both compounds. The structural packing along the *c*-axis is determined both by the M —O bond length, which fixes the distance between OH groups in an octahedral sheet, and by the strength of interactions in the interlayer spacing.

The values of thermal coefficients u_{ij} of H atoms, calculated in the harmonic one-site model, are almost equal for both compounds (Table 2). The very large value of u_{11} has to be correlated to the existence of three minimum energy positions for the H atom. The deviation from the $2d$ symmetry site is almost equivalent for both compounds ($\bar{\alpha} \approx 9.5^\circ$, Fig. 1). Unlike $\text{Ca}(\text{OH})_2$, the refinements with an anharmonic thermal motion for the H atom in $\text{Mg}(\text{OH})_2$ are not significant, probably because of data sets which are not sufficiently extended in $\sin \theta/\lambda$. For $\text{Ca}(\text{OH})_2$ the results obtained at room temperature show that the maximum probability density for the H atom is situated on the symmetry site; on the other hand, at 80 K thermal energy is much reduced and the occupation rate of three-disordered sites is increased such that the maximum H-atom probability density is no more on the symmetry site (Desgranges *et al.*, 1993).

This study was supported by the Region Bourgogne. We are grateful to Professor F. Freund, San Jose University, for supplying the single crystal of $\text{Mg}(\text{OH})_2$.

References

- Brindley, G. W. & Kao, C. C. (1984). *Phys. Chem. Miner.* **10**, 187–191.
- Busing, W. R. & Levy, H. A. (1957). *J. Chem. Phys.* **26**, 563–568.
- Ceccarelli, G. A., Jeffrey, A. & Taylor, R. (1981). *J. Mol. Struct.* **70**, 255–271.
- Delapalme, A. (1985). Internal Report, D PhG. SDN/85/59, LLB-CEN Saclay.
- Desgranges, L., Grebille, D., Calvarin, G., Chevrier, G., Floquet, N. & Niepce, J. C. (1993). *Acta Cryst.* **B49**, 812–817.
- Greaves, C. & Thomas, M. A. (1986). *Acta Cryst.* **B42**, 51–55.
- Krishnan, R. S., Srinivasan, R. & Devanarayannan, S. (1979). *Thermal Expansion of Crystals*. Oxford: Pergamon Press.
- Kruger, M. B., Williams, Q. & Jeanioz, R. (1989). *J. Chem. Phys.* **91**(10), 5910–5915.
- Partin, D. E., O'Keefe, M. & von Dreele, R. B. (1994). *J. Appl. Cryst.* **27**, 581–584.
- Shannon, R. D. (1974). *Physics and Chemistry of Minerals and Rocks*, pp. 403–431. New York: Wiley Interscience Publications.
- Zigan, F. & Rothbauer, R. (1967). *Neues Jahrb. Mineral. Montash.* pp. 137–143.
- Zucker, U. H., Perenthaler, E., Kuhs, W. H., Bachmann, R. & Schulz, H. (1983). *J. Appl. Cryst.* **16**, 358.